

Universal Anisotropy in Force Networks under Shear

Srdjan Ostojic,^{1,*} Thijs J. H. Vlugt,² and Bernard Nienhuis¹

¹*Institute for Theoretical Physics, Universiteit van Amsterdam,
Valckenierstraat 65, 1018 XE Amsterdam, The Netherlands*

²*Condensed Matter and Interfaces (CMI), Utrecht University,
P.O.Box 80.000, 3508 TA Utrecht, The Netherlands*

(Dated: July 18, 2021)

Abstract

Scaling properties of patterns formed by large contact forces are studied as a function of the applied shear stress, in two-dimensional static packings generated from the force network ensemble. An anisotropic finite-size-scaling analysis shows that the applied shear does not affect the universal scaling properties of these patterns, but simply induces different length scales in the principal directions of the macroscopic stress tensor. The ratio of these length scales quantifies the anisotropy of the force networks, and is found not to depend on the details of the underlying contact network, in contrast with other properties such as the yield stress.

PACS numbers: 45.70.-n, 45.70.Cc, 46.65.+g

Aggregates of macroscopic particles such as granular materials, foams and emulsions are often found in a disordered, solid-like state whose mechanical properties have attracted much attention in recent years [1, 2, 3, 4, 5, 6, 7, 8, 9, 10, 11, 12, 13]. Under external stresses, these systems present a non-zero yield threshold which is solely due to the intricate network formed by contact forces between particles. One of the most remarked features of these highly disordered *force networks* is the tendency for large forces to align and form branching *force chains*. When these appear in response to an external stress, such as a global shear, their spatial inhomogeneity is most striking [6, 7, 8]. As the applied shear stress is increased, the large forces orient in a preferred direction, and the force network becomes more and more anisotropic (c.f. Fig. 1), up to the point where the applied stress can no longer be sustained, and the packing yields. While this qualitative picture has been long established, due to a lack of appropriate analytic and numerical tools, quantitative studies of packings under static shear have been few [6, 7, 8, 9, 11].

Recently, a novel characterization has been introduced for the geometrical patterns formed by large forces in isotropically compressed force networks [13]). The patterns, displayed by molecular dynamics (MD) simulations of granular packings, turned out to have scaling properties which are independent of the pressure, polydispersity and friction. An intriguing question is whether an analysis of scaling properties can provide insight into the organization of force networks in packings under shear. This is a much more difficult problem.

Creating static packings under shear with MD is seriously hindered by local rearrangements that seem to prevent the system from reaching a clear mechanical equilibrium. To allow for systematic examinations of the effects of shear, it has been proposed [10, 11] to ignore the microscopic rearrangements of the grains, and study the ensembles of force networks allowed on a given contact network, as function of macroscopic stresses. This purely statistical approach was found to account well for the properties of packings under shear such as the existence of a yield threshold [11], as well as for the scaling properties of clusters of large forces in packings without shear [13]. It also describes remarkably well the distribution of force magnitudes [10, 11, 12] and the response to an external overload [14].

In this Letter, we study the geometry of patterns of large forces in two-dimensional, static packings under shear generated from the force network ensemble. We find that applying shear stress leaves unchanged the universal scaling properties of the patterns, but introduces two different length scales in the two directions of principal stress axes. We characterize the

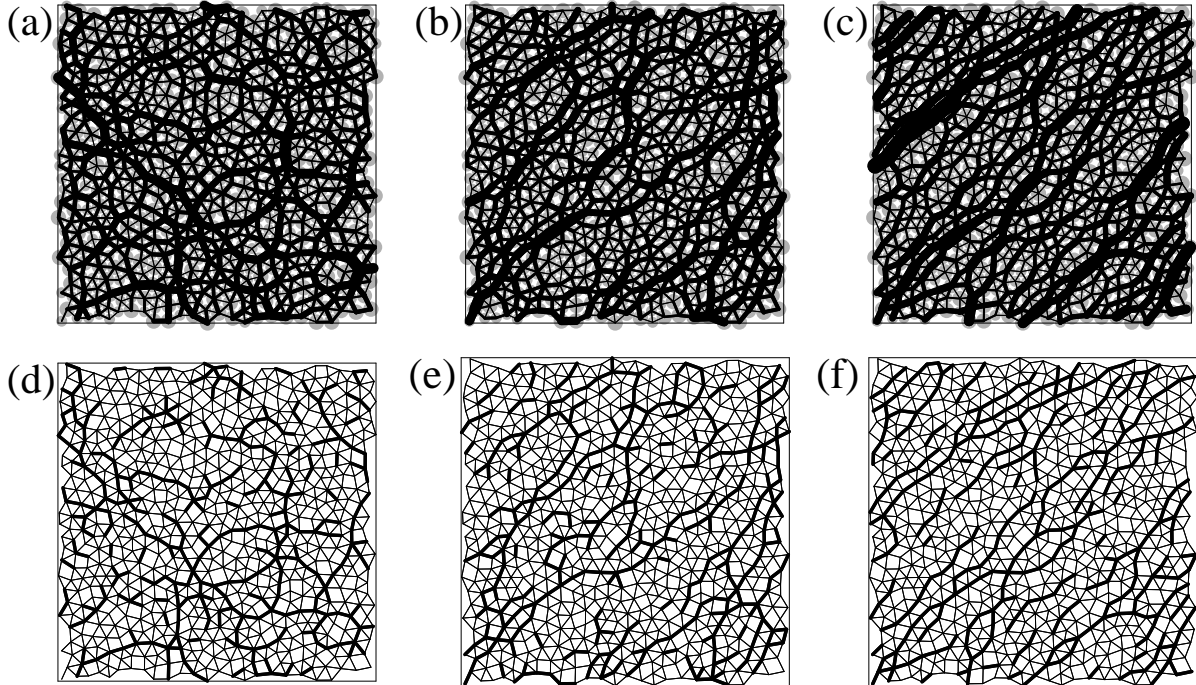


FIG. 1: Effect of shear on force networks: (a-c) Force networks obtained from the force ensemble, for three different values of shear: (a) $\tau = 0$, (b) $\tau = 0.2$, (c) $\tau = 0.4$. The forces are represented as bonds connecting centers of grains of contact, the width of each bond being proportional to the magnitude of the force. The underlying contact network is the same for all values of τ . (d-f) Clusters of forces larger than a threshold f (bold bonds), obtained for f close to the critical value.

anisotropy of the force networks by the ratio r of these length scales. An anisotropic finite-size scaling analysis allows us to determine r as function of the applied shear stress τ and the coordination number of the packing. In contrast with other properties such as the yield stress, $r(\tau)$ turns out to be independent of the underlying contact geometry, and thus provides a universal characterization of shear-induced anisotropy.

Force networks— To study systematically the influence of the shear stress on the geometry of large forces we examined force networks generated from the force network ensemble pertaining to packings of frictionless, non-attracting particles. This approach relies on the fact that in a typical packing, the number of unknown contact forces is larger than the number of equations for mechanical balance [10]. For a given, fixed, contact geometry, the force network ensemble consists of all force networks with repulsive contact forces in mechanical

balance on each grain, and consistent with the tensor σ of applied macroscopic stress. The considered contact networks are isotropic, and the coordinates are such that the pressure is isotropic, i.e. $\sigma_{xx} = \sigma_{yy}$, while the dimensionless shear stress $\tau = \sigma_{xy}/\sigma_{xx}$ is varied.

The ensemble is sampled numerically using two different methods : (i) the wheel-move algorithm [12] for ordered, hexagonal packings ($z = 6$); (ii) the procedure outlined in [11] for disordered packings of various coordination numbers z . Both methods efficiently generate very large packings (10^5 and $5 \cdot 10^4$ particles respectively), from which smaller sub-systems were extracted and analyzed. Note that the ensemble is non-empty only for τ smaller than a maximal value $\tau_{max}(z)$, which has been identified as the yield stress [11].

Force chains— To study the geometry of patterns formed by large forces, we follow the method introduced in [13], which we here briefly recall and then extend to packings under shear. The force network in a packing of frictionless particles can be represented as a set of bonds connecting grains in contact, where each bond carries the magnitude of the corresponding contact force (c.f. Fig. 1 (a-c)). A natural way to isolate the force chains in such a network is to choose a threshold f , and consider only the subgraph formed by bonds carrying forces larger than f (c.f. Fig. 1 (d-f)). Varying this threshold allows to study patterns of large forces at different scales: for small values, most of the grains remain connected, but as the threshold is increased, the extracted subgraph breaks into disconnected clusters. The extent of each chain of forces larger than the threshold can be characterized by the size of the corresponding cluster, quantified by the number s of mutually connected bonds.

In an ensemble of packings, a statistical description of the fluctuating patterns of large forces is given by the statistics of the clusters obtained at different thresholds. Following the methods of percolation theory [15], the geometry of an ensemble of packings can be characterized by $P(s, f)$, the number (per bond) of clusters of size s at the threshold f . For packings under isotropic pressure, it is moreover natural to describe the clusters by a single characteristic length, the cluster correlation length $\xi(f)$, which corresponds to the typical linear size of the clusters at a given threshold (not considering clusters percolating through the whole system).

Scaling analysis—Analogously to percolation and other lattice models of critical phenomena, the system is critical around the value f_c of the threshold above which no infinite cluster is found. At this value, $\xi(f)$ diverges as $|f - f_c|^{-\nu}$, and $P(s, f)$ becomes a power-law,

its moments $\langle s^n \rangle$ diverging as powers of $\xi(f)$: $\langle s^n \rangle \sim \xi^{\phi_n}$. For systems of finite size, the correlation length is naturally bounded by the linear size of system, L , and for ξ comparable to L , the behavior of $\langle s^n \rangle$ is given by a scaling function of L/ξ [16, 17]:

$$\langle s^n(f, L) \rangle \sim L^{\phi_n} \Sigma_n[(f - f_c)L^{1/\nu}], \quad (1)$$

where ϕ_n and ν are universal critical exponents, and Σ_n universal scaling functions. For force networks under isotropic pressure, $\phi_2 = 1.89$, $\nu = 1.65$, and Σ_2 is independent of pressure, polydispersity, friction and force law [13]. From now on, we will only consider the case $n = 2$, and omit the indices n in the right-hand-side. Note that the scaling function Σ_2 varies smoothly and displays a single maximum close to zero.

Equation (1) assumes that the size of the examined domains is isotropic. In the following, we will need to consider rectangular domains of size $L_1 \times L_2$, in which case the scaling function Σ also depends on the aspect ratio L_2/L_1 . Considering only the maximum of $\langle s^2(f, L_1, L_2) \rangle$ with respect to f , which is equivalent to looking only at the behavior at the effective critical point, Eq. (1) reduces to

$$\langle s^2(L_1, L_2) \rangle_{max} = L_2^{\phi} \bar{\Sigma} \left(\frac{L_1}{L_2} \right). \quad (2)$$

The scaling function $\bar{\Sigma}(x)$ simply expresses the fact that if $L_1 \ll L_2$, the effective correlation length is set by L_1 , so that $\langle s^2 \rangle_{max} \sim L_1^{\phi}$, and correspondingly if $L_2 \ll L_1$, $\langle s^2 \rangle_{max} \sim L_2^{\phi}$. We therefore have (with $y = L_1/L_2$)

$$\bar{\Sigma}(y) \sim \begin{cases} y^{\phi} & \text{for } y \ll 1 \\ 1 & \text{for } y \gg 1 \end{cases} \quad (3)$$

For $L_1 \sim L_2$, there is a crossover between the two asymptotic trends, and the precise behavior is determined by the scaling function.

Shear-induced anisotropy— The analysis presented so far pertains to the case of isotropic pressure. In packings under shear, the force networks become increasingly anisotropic as the shear stress is increased, the large forces aligning preferentially in the direction of the maximal stress axis (cf. Fig. 1). In consequence, close to the percolation threshold the clusters can no longer be described by a single length scale. Instead two correlation lengths ξ_M and ξ_m must be distinguished, in the direction of maximal and minimal stress axes respectively. In principle, at criticality these two length scales could diverge with two different exponents ν_M and ν_m . A finite-size scaling analysis as in [13], but now varying independently the

system sizes L_M and L_m in the directions of principal stresses, shows that $\nu_M = \nu_m = \nu$, the exponents ϕ and ν being equal to those of isotropically compressed packings.

Although they diverge with the same exponent, the values of the correlation lengths ξ_M and ξ_m clearly differ. This implies that, to leading order,

$$\xi_M = \xi_M^{(0)} |f - f_c|^{-\nu} \quad \text{and} \quad \xi_m = \xi_m^{(0)} |f - f_c|^{-\nu}. \quad (4)$$

where the length scales $\xi_M^{(0)}$ and $\xi_m^{(0)}$ depend on the shear stress τ but not on the threshold f . In the language of critical phenomena, this situation is called *weakly anisotropic scaling*, as opposed to the case where the two correlation-length exponents differ [17].

To quantify the anisotropy of force networks as function of shear stress, from Eq. (4), it appears natural to use the anisotropy ratio $r(\tau)$ defined as

$$r(\tau) = \frac{\xi_m^{(0)}}{\xi_M^{(0)}}. \quad (5)$$

Clearly, for $\tau = 0$, $r = 1$, and as τ is increased, r decreases below one.

The anisotropy ratio r as function of τ can be determined using an anisotropic scaling analysis. The central observation is that, in the context of conventional critical phenomena, a weakly anisotropic system can be made isotropic simply by rescaling the lengths in the two directions of principal axes. In the present setting, this property suggests that if the actual lengths L_M and L_m are replaced by properly rescaled effective lengths \tilde{L}_M and \tilde{L}_m , the scaling properties of the sheared force networks should be identical to those of isotropically compressed networks. This property allows us to determine the ratio of length scales $\xi_M^{(0)}$ and $\xi_m^{(0)}$.

More specifically, the scaling of the maximum of $\langle s^2 \rangle$ is described by Eq. (2) with an additional dependence on the shear stress τ in the right hand side. Our hypothesis is that the scaling function $\bar{\Sigma}$ does not depend explicitly on τ , and that the anisotropy can be eliminated simply by replacing L_M and L_m by rescaled lengths \tilde{L}_M and \tilde{L}_m given by

$$\tilde{L}_M = b_M(\tau) L_M \quad \text{and} \quad \tilde{L}_m = b_m(\tau) L_m \quad (6)$$

with $b_M = 1/\xi_M^{(0)}$ and $b_m = 1/\xi_m^{(0)}$, and therefore $r(\tau) = b_M/b_m$. Substituting into Eq. (2), the scaling relation becomes

$$\langle s^2(L_M, L_m, \tau) \rangle_{max} = (b_m L_m)^{\phi \bar{\Sigma}} \left(\frac{b_M L_M}{b_m L_m} \right). \quad (7)$$

where the dependence on τ occurs only through the scale factors b_m and b_M .

The validity of the scaling relation (7) can be checked directly from the numerical data. Fig. 2 illustrates the behavior of $\langle s^2 \rangle_{max}$ as function of L_m , for three different values of τ , and in each case three different values of L_M . For fixed L_M and τ , as L_m increases, at first a clear power-law can be observed. For larger values of L_m , a crossover occurs and $\langle s^2 \rangle_{max}$ reaches a plateau. As L_M is increased, the behavior in the scaling regime is unchanged, but the crossover occurs at larger L_m , and the value of the plateau increases. According to Eq. (2), the value of the crossover should scale as L_M , and the value of the plateau as L_M^ϕ . Rescaling both axes appropriately, the data for different L_M indeed collapse on the same curves as shown in Fig. 2 (b).

For different values of the shear stress, the exponents in the scaling regimes appear to be identical, however the prefactors of the power laws clearly depend on τ . From Eq. (7), these prefactors correspond to b_M and b_m , which can thus be determined respectively from the value reached at the plateau and the intercept of the power law. Replacing L_M and L_m by rescaled lengths \tilde{L}_M and \tilde{L}_m defined in Eq. (6), if the scaling function $\bar{\Sigma}$ is independent of τ , all the data must collapse on a single curve. Note that as τ is increased, the crossover occurs at smaller L_m , and the domain of power-law scaling shrinks, so that b_m can be extracted only for τ sufficiently smaller than the yield stress τ_{max} (beyond which the force network ensemble is empty).

Fig. 3 displays the results obtained for all considered values of shear stress τ , on several packing geometries of different coordination number z ($z = 6$ corresponds to the ordered hexagonal case, while the other packings are disordered). All the data clearly collapse on the same curve, in agreement with the hypothesis that the scaling function does not depend on τ . As postulated, a simple rescaling of the length scales in the two directions of anisotropy is thus sufficient to recover isotropic scaling in force networks under shear. The inset of Fig. 3 displays the anisotropy parameter $r = \frac{b_M}{b_m}$ as function of τ . Unexpectedly, $r(\tau)$ appears to be independent of the coordination number and geometry of the underlying contact network.

Discussion— Our results show that applying an external shear stress on a force network does not affect the universal scaling properties of the force chains, but only induces two different length scales in the directions of the two principal stress axes. While these typical lengths and their ratio r are not a priori expected to be universal, we find that they

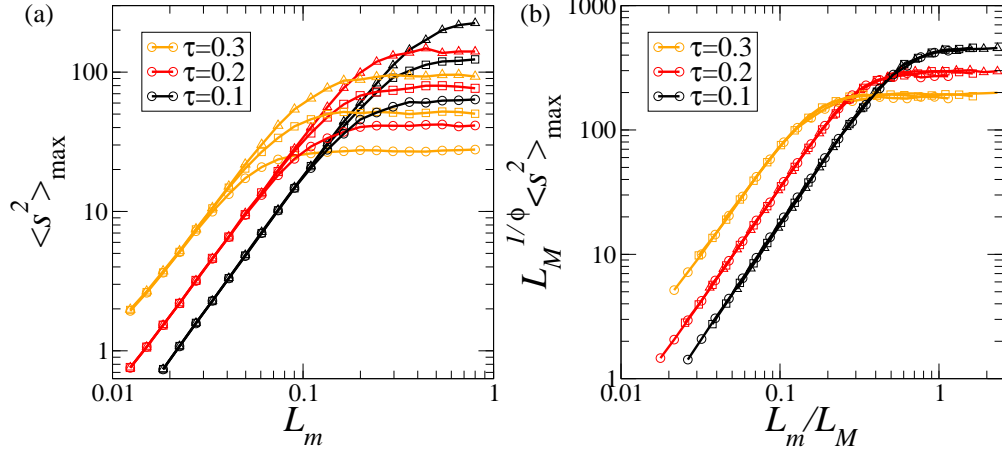


FIG. 2: (color online) Scaling of the maximum of the second moment of cluster sizes: (a) $\langle s^2 \rangle_{\max}(L_M, L_m)$ as function of L_m . Three different values of L_M are represented with circles, squares and triangles, while three different values of the shear stress are shown in three different colors. The displayed data corresponds to hexagonal packing of disks, i.e. $z = 6$. (b) Collapses of data corresponding to same τ , obtained by rescaling the axes by L_M . The curves are colored in the order of the legend.

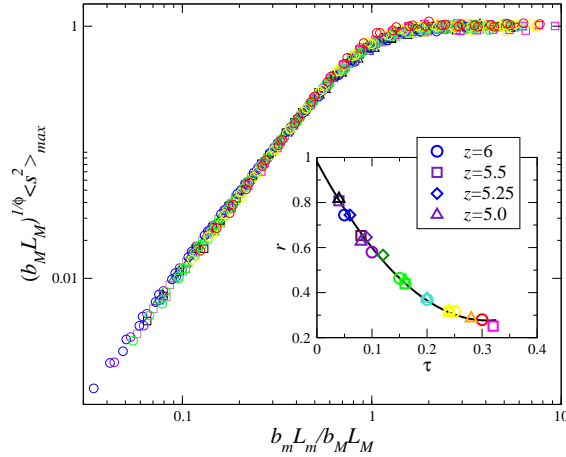


FIG. 3: (color online) The anisotropic scaling function $\bar{\Sigma}$ (cf. Eq. (2)): collapse of data obtained for different values of shear stress τ and different packing geometries. Each symbol corresponds to data for a different coordination number z ($z = 6$: regular, hexagonal packing, already displayed in Fig. 2; all others: disordered packings). Each value of τ is represented by a different color. The inset shows the anisotropy parameter $r = \frac{b_M}{b_m}$ as function of τ , for different z . The black solid line is a quadratic fit.

are identical for various contact networks we considered, which include the regular hexagonal packing, and disordered networks of different coordination numbers, and in this sense universal.

An important remaining question is the behavior close to the yielding point. If yielding is analogous to a phase transition, as suggested by the jamming picture [4, 5], it could be expected that close to it a cross-over occurs, and the scaling properties of clusters of large forces change significantly. The value of the yield stress τ_{max} was found to be strongly dependent on the coordination number z of the contact network [11]. On the other hand, we find that $r(\tau)$ is completely independent of z up to $\tau_{max}(z)$. This observation suggests the absence of any diverging or vanishing length scale which would accompany the cross-over close to τ_{max} . Moreover, we have not observed any dramatic change in the scaling properties close to τ_{max} , but additional work is necessary to clarify these issues.

TJHV acknowledges financial support from the Netherlands Organization for Scientific Research (NWO-CW) through a VIDI grant. SO is financially supported by the Dutch research organization FOM.

* Present address: Laboratoire de Physique Statistique, Ecole Normale Supérieure, 24, rue Lhomond, 75231 Paris Cedex 05, France

- [1] H. M. Jaeger, S. R. Nagel, and R. P. Behringer, *Rev. Mod. Phys.* **68**, 1259 (1996).
- [2] P.-G. de Gennes, *Rev. Mod. Phys.* **71**, 374 (1999).
- [3] J.-P. Bouchaud, in *Les Houches, Session LXXVII*, edited by J. Barrat (EDP Sciences, 2003).
- [4] A. J. Liu and S. R. Nagel, *Nature* **396**, 21 (1998).
- [5] A. Liu and S. Nagel, *Jamming and rheology* (Taylor & Francis, 2001).
- [6] F. Radjai, D. E. Wolf, M. Jean, and J.-J. Moreau, *Phys. Rev. Lett.* **80**, 61 (1998).
- [7] J. Geng, G. Reydellet, E. Clement, and R. P. Behringer, *Physica D* **182**, 274 (2003).
- [8] T. S. Majmudar and R. P. Behringer, *Nature* **435**, 1079 (2005).
- [9] A. Atman and *et al.*, *J. Phys. Cond. Mat.* **17**, S2391 (2005).
- [10] J. H. Snoeijer, T. J. H. Vlugt, M. van Hecke, and W. van Saarloos, *Phys. Rev. Lett.* **92**, 054302 (2004).
- [11] J. H. Snoeijer, W. G. Ellenbroek, T. J. H. Vlugt, and M. van Hecke, *Phys. Rev. Lett.* **96**,

- 098001 (2006).
- [12] B. Tighe and *et al.*, Phys. Rev. E **72**, 031306 (2005).
 - [13] S. Ostojic, E. Somfai, and B. Nienhuis, Nature **439**, 828 (2006).
 - [14] S. Ostojic and D. Panja, Phys. Rev. Lett. in press , cond-mat/0606349.
 - [15] D. Stauffer and A. Aharony, *Introduction to Percolation Theory* (Taylor & Francis, 1991).
 - [16] V. Privman, *Finite Size Scaling and Numerical Simulations of Statistical Physics* (World Scientific, 1990).
 - [17] K. Binder and J.-S. Wang, J. Stat. Phys. **55**, 87 (1989).